Journal of the Korean Society of Oceanography
Vol. 33, No. 3, pp. 71—79, September 1998

Silty Tidal Rhythmites from the Upper Pleistocene Sedimentary Sequence, Western Coast of Korea

YONG AHN PARK AND KYUNG SIK CHOI
Department of Oceanography, Seoul National University, Seoul 151-742, Korea

Silty tidal rhythmites were found from the upper Pleistocene sequence unconformably overlain by the Holocene tidal deposits within the macrotidal coastal zone of Youngjong Island, western coast of Korea. The rhythmites occur as vertically accreted, parallel and planar laminae that are 0.1—2.5 mm in thickness. Each lamina grades from coarse silt (mean grain size: 5—6.5 ϕ) at the lower part into fine silt to mud (mean grain size: 6—7.5 ϕ) at the upper part. The rhythmites can be classified into two types based on the patterns in laminar thickness variation. Type I is a bundle of 12—20 laminae in which laminar thickness varies sinusoidally. Type II is an alternation of thick and thin laminae as a couplet. Type I is inferred as a product of varying tidal energy during a semimonthly (neap-spring) tidal cycle, in which thicker laminae were deposited during spring tides and thinner laminae were formed during neap tides. Type II is interpreted to have been formed by asymmetric semidiurnal tidal currents in association with diurnal inequality, whereby thick lamina of each couplet represents dominant tidal current and the thin lamina reflects subordinate tidal current.

INTRODUCTION

Studies on the recognition of tidal rhythmites have significantly improved the sophisticated reconstruction of paleodepositional environment (Brown *et al.*, 1990; Williams, 1991; Chan *et al.*, 1994; Greb and Archer, 1995; Tessier *et al.*, 1995; Kvale and Archer, 1996). Especially in estuarine settings, tidal rhythmites are particularly useful in distinguishing subenvironments along the fluvial to marine transition because of their sensitivity to variations in physical and biological processes (Dalrymple *et al.*, 1991; Lanier *et al.*, 1993; Archer *et al.*, 1994; Feldman *et al.*, 1995). Since tidal rhythmites demonstrate high-resolution and continuous records of tidal sedimentation related to the hierarchy of tidal cyclicities (semidiurnal, diurnal, semimonthly, monthly, semiannual, annual), they have been regarded as an unambiguous indicator of tide-influenced depositional settings (Kvale and Archer, 1991; Tessier, 1993; Kvale *et al.*, 1995).

Recognition of tidal cyclicities from the laminar structure provides unique criteria for distinguishing tidal rhythmites from other non-tidal rhythmic deposits formed in various depositional settings (*i.e.* lake, shelf, delta, *etc.*). Identification of tidal rhythmites is convinced only when cyclicities similar to known tidal cycles are established via sequential measurement of laminar thickness. Such correlations have been achieved by both field observations in macrotidal estuaries (Dalrymple and Makino, 1989; Dalrymple *et al.*, 1991; Tessier, 1993; Archer and Johnson, 1997) and simulations from modern tidal data (Archer *et al.*, 1991, 1995; Kvale *et al.*, 1995; Archer and Johnson, 1997).

This paper aims to describe the nature of silty rhythmites from the upper Pleistocene sequence unconformably overlain by the Holocene transgressive tidal deposits within the macrotidal coastal zone of the Youngjong Island, western coast of Korea. To reveal the origin of the cyclic laminar structure, we conducted microscopic analysis for the textural characters of lamina as well as sequential measurement of laminar thickness.

STUDY AREA

Macrotidal flats are extensively developed around the Youngjong Island off the western coast of Korea (eastern margin of the Yellow Sea), which are disconnected from the mainland by a conspicuous channel of more than 20 m deep (Fig. 1). At spring tides, tidal range reaches up to more than 8 m and tidal current attains its maximum velocity

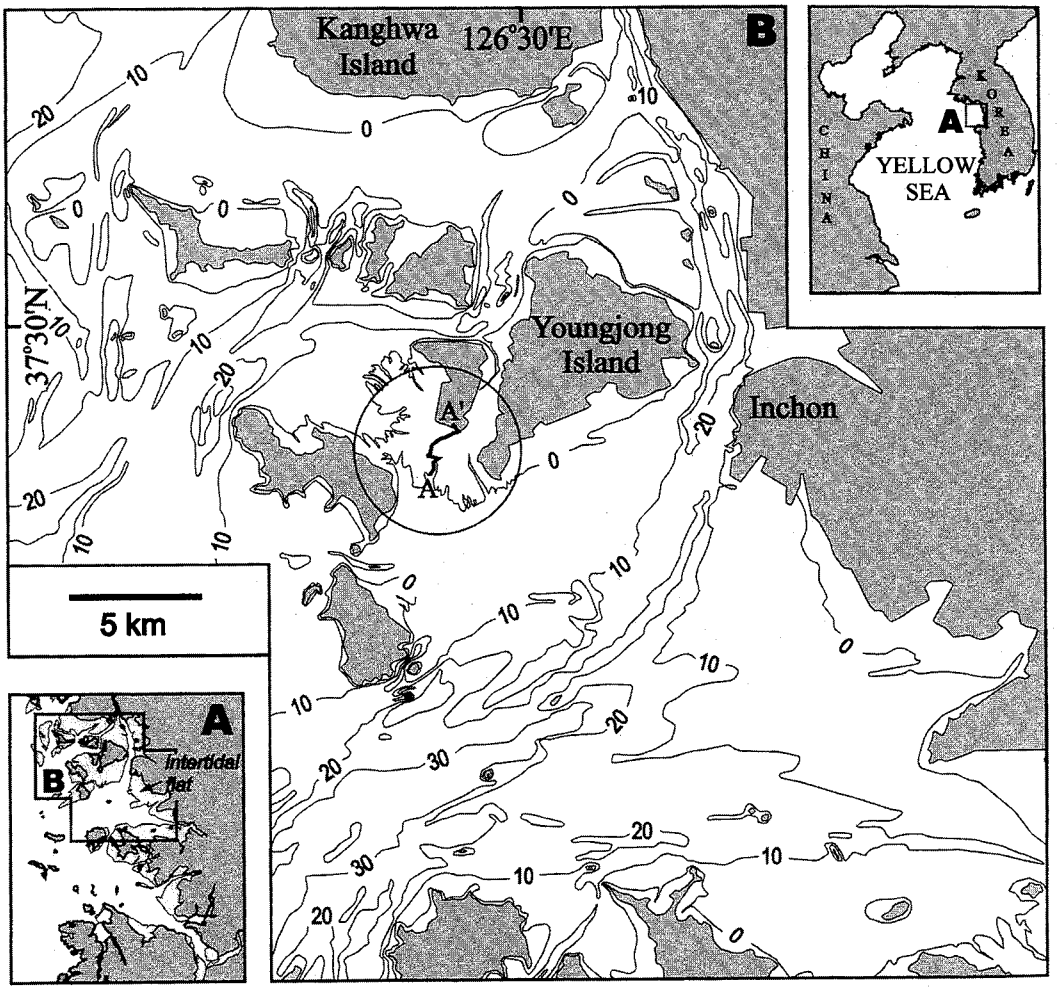

Fig. 1. Physiographic map of the study area. Depths are in meters below mean sea level.

of about 3 m/s during ebb tides. Dendritic tidal channels and creeks are well developed on the tidal flat. Tidal flat surface is dominated by sandy silt to mud, but gradually replaced with silty sand and sand toward the main channels. Gravels are found in the bottom of the channel between Inchon and Youngjong Island. Overall distribution of surface sediments shows a shoreward-fining trend (Lee *et al.*, 1985). The Han River situated about 40 km northeast of the study area is the major source of suspended sediment. Currently, the study area has been reclaimed for the construction of an airport since 1992.

Coastal sequence around the Youngjong Island consists of six lithostratigraphic units (Choi and Park, 1996; Fig. 2). Holocene tidal deposits comprise the uppermost part of sequence and develope as thick as 15 m. Early Holocene siderite-rich stiff muds are overlain by the Holocene tidal deposits with an erosive contact (transgressive surface). Late Pleistocene, weathered tidal deposits occur beneath the early Holocene siderite-rich stiff muds and contain typical cryogenic structures indicating prolonged pedogenic processes under the cold and dry climate. Late Pleistocene tidal deposits as thick as 20 m are overlain by the weathered tidal deposits with a gradational contact. Unlike to Holocene tidal deposits, they are slightly bioturbated and contain various kinds of tide-influenced structures such as flaser, wavy and lenticular bedding, herringbone cross-bedding and reactivation surfaces with mud drapes, though marine microfossils have not been observed yet. Organic-rich muds and basal gravelly sands underlie the late Pleistocene tidal deposits and unconformably overlie Jurassic basement rock.

MATERIALS AND METHODS

More than 200 standard penetration test (SPT) samples were collected from 15 boreholes which

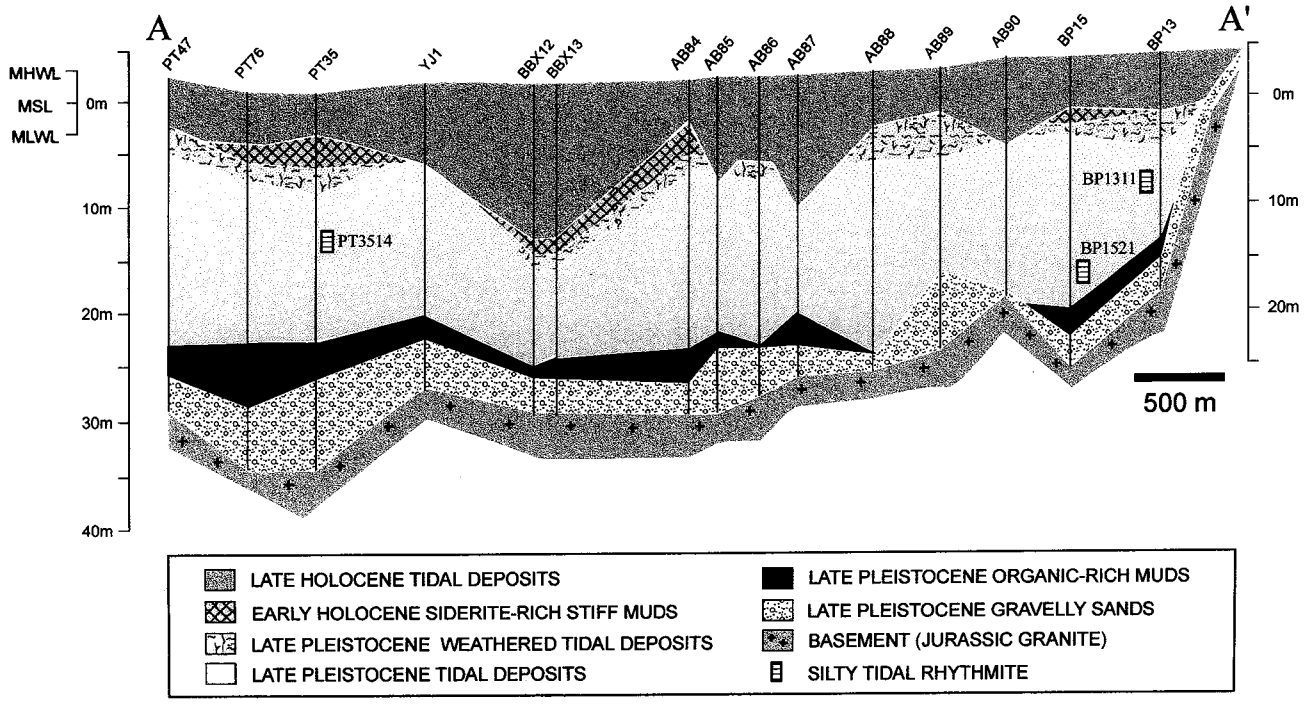

Fig. 2. Schematic cross-section of transect A-A' in Fig. 1, showing the lateral and vertical relationships of six litho-stratigraphic units with the location of SPT samples displaying silty tidal rhythmites.

penetrated sedimentary sequences as deep as 40 m into the basement rock. They were sliced lengthwise into halves and photographed. Three SPT samples (PT3514, BP1311 and BP1521) were chosen and impregnated with Spurr resin (Jim, 1985). Thin sections were prepared for the microscopic observa-

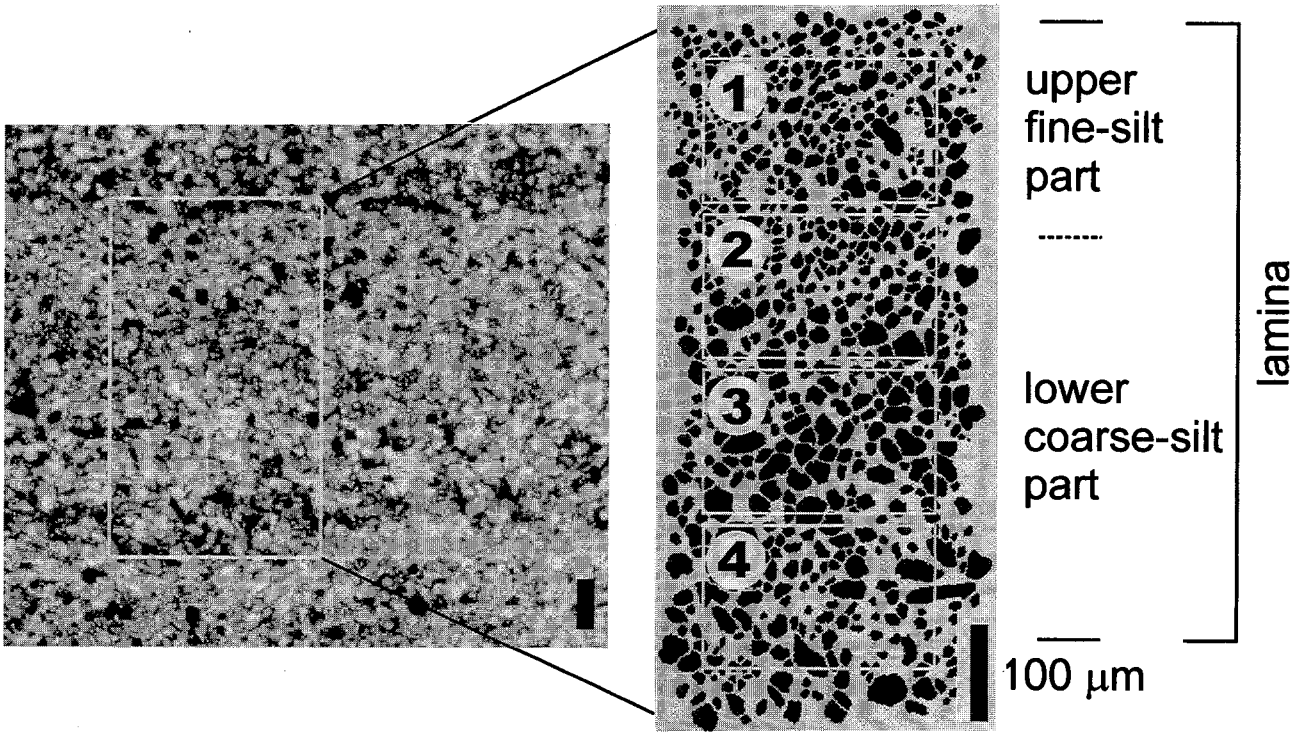

Fig. 3. Photomicrograph and sketch of a normally graded lamina composed of fine silt to mud at the upper part and coarse silt at the lower part. Grain size distribution for each numbered box appears in Fig. 4. Scale bars are 100 μm.

tion of laminar structure. Laminar thickness was precisely and sequentially measured under polarizing microscope with varying magnifications from ×50 to ×200. Textural composition of each lamina was quantitatively analyzed by an image analyzing program (BMI Plus of BMI Co.).

RESULTS

Sedimentary characteristics of silty rhythmites

Silty rhythmites occur only in the late Pleistocene tidal deposits whose vertical distribution depth ranges from 6 to 25 m below the present mean sea level (Fig. 2). They are composed of parallel and planar laminae, each of which grades from coarse silt (mean grain size: 5—6.5 ϕ) at the lower part into fine silt to mud (mean grain size: 6—7.5 ϕ) at the upper part (Figs. 3 and 4). Individual laminae range in thickness from 0.1 to 2.5 mm. They are laterally persistent and relatively uniform in thickness only with undulatory submillimeter-scale relief (< 0.2 mm). Sand grains are rare, being restricted to those laminae of more than 2 mm thick. Quartz is the most dominant constituent mineral, comprising more than 70%. Feldspar occurs in lesser amount, *ca.* 20%. Horizontally oriented flaty minerals such as mica are concentrated in the upper fine-silt part. Slightly inverse gradings are developed near the base of the lower coarse-silt part in which sediments are poorly sorted due to the presence of aggregated lumps of fine-grained particles (very fine silt to clay) incorporated from the underlying lamina. Laminar boundaries are sharp but not erosional.

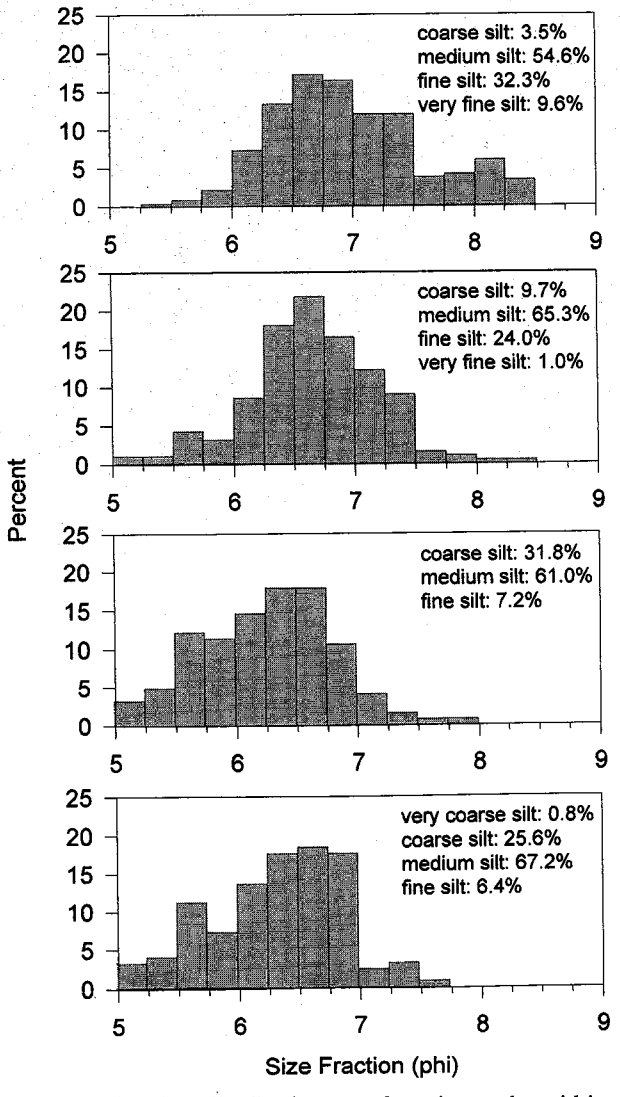

Fig. 4. Grain size distributions at four intervals within a graded lamina. Note grain size distribution shifts toward fine fraction from base to top.

Plots of laminar thickness reveal two types of variations. Type I is the progressive increase and following decrease of laminar thickness over 12—20 laminae (Figs. 5 and 6). This cyclicity also causes to alternate between sandier and muddier intervals over a vertical distance of 0.7—2.5 cm. In muddier portions of the cycles, laminae are generally thin and often merge. In sandier portions of the cycles, each lamina is typically over 1 mm thick and shows sharp bases. Type II consists of the alternation of thick and thin laminae as a couplet, giving a saw-tooth appearance (Fig. 7). This pattern repeats as many as 6—7 times and is amalgamated on the gradual variation of laminar thickness (Type I).

Evidence of tidal sedimentation

Microscopic observation of laminar structures provides some evidence on the origin of silty rhythmites. Based on the detailed and sequential measurements of grain size distribution of laminae, normal grading pattern is clearly demonstrated (Figs. 3, 4 and 8). Such pattern seems to be more distinct as the lamina becomes thick (Fig. 8). A normally graded lamina is interpreted to have been formed during a single current cycle. Lack of both cross laminae and coarse grains indicates suspension fallout sedimentation rather than migration of bedforms. As lamina becomes thin upward, both mean grain size and percentage of 5 ϕ fraction (the coarsest fraction) decrease accordingly (Fig. 8 and Table 1). Mean grain size at the lower part of each

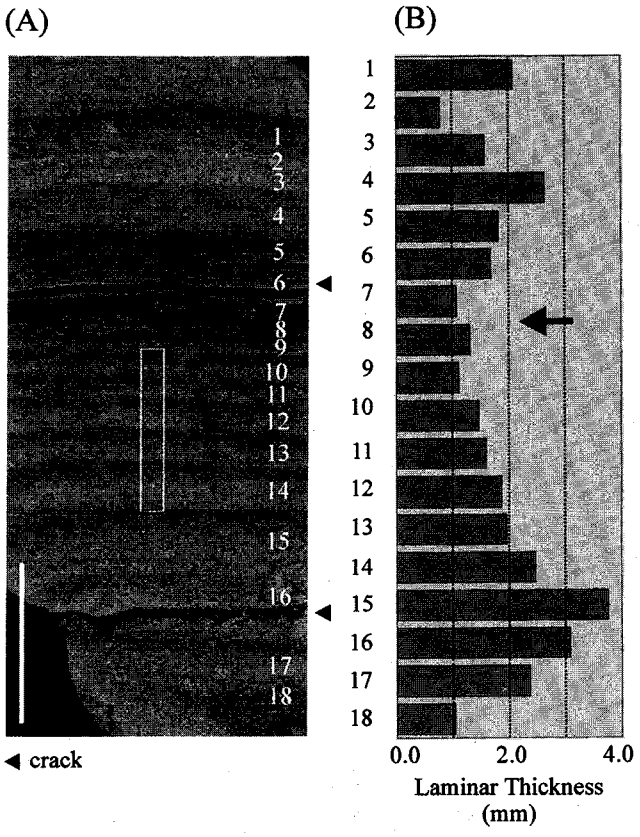

Fig. 5. (**A**) Photograph of cored sample PT3514 showing a gradual increase-and-decrease of laminar thickness. Scale bar is 1 cm. Refer to Fig. 8 for photomicrograph of box area in the middle of figure. (**B**) Plot of laminar thickness against laminar number. Inferred neap stage is indicated by an arrow. See Fig. 2 for sample location.

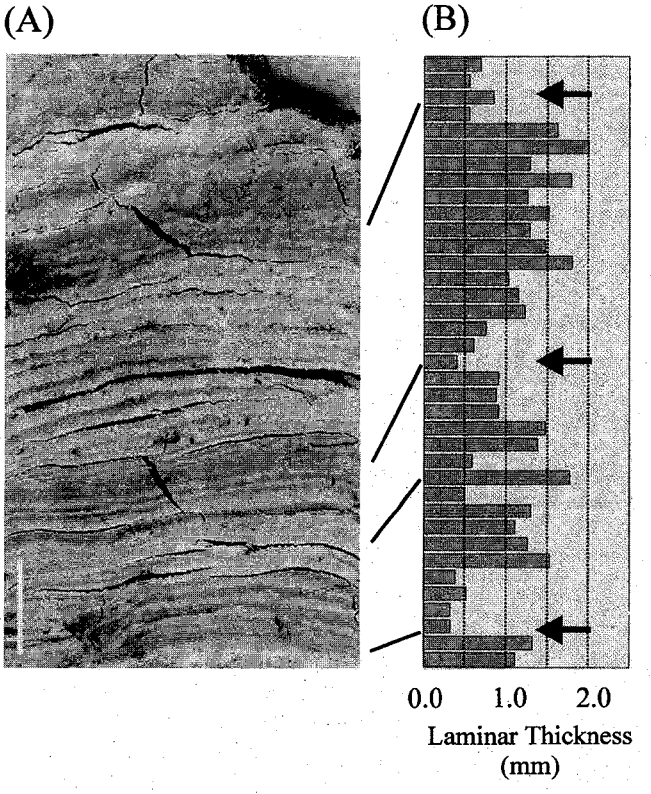

Fig. 6. (**A**) Photograph of cored sample BP1311 showing sinusoidal changes of laminar thickness. Scale bar is 1 cm. (**B**) Plot of laminar thickness against laminar number. Inferred neap stages are indicated by arrows. See Fig. 2 for sample location.

lamina shows a marked decrease from 25.9 μm at the lowermost and thickest lamina (Lamina 1 in Fig. 8) to 15.6 μm at the uppermost and thinnest lamina (Lamina 5 in Fig. 8). Similarly, the variation of percentage of 5 ϕ fraction mimics the pattern of mean-grain-size variation, comprising 25% at Lamina 1, 6% at Lamina 3 and 3% at Lamina 5. The thicker lamina is the coarser and *vice versa*. Since net sediment accumulation rate is known to be proportional to the cube of excess velocity (Nio and Yang, 1991), progressive changes in laminar thickness and the related changes in textural composition represent gradual variation of current velocities during the laminar formation.

The gradual increase and thereafter sinuous decrease in laminar thickness over 12—20 laminae is interpreted to reflect the semimonthly change of tides, namely, neap-spring cycle. As the current velocity increases, more and coarser sediments are entrained and transported to deposit thicker and coarse-grained lamina. Thus, the interval of coarser and thicker laminae presumably represents spring tides, when stronger tidal currents are generated. In the same context, finer and thinner laminae reflect relatively weak tidal currents during neap tides. Very fine plant stems and rootlets (less than 1 mm in diameter) common in the thinner and muddier laminae are also indicative of relatively low energy conditions during neap tides.

The alternation of thick and thin laminae as a pairing can be made by a marked diurnal inequality in heights between successive high tides in a semidiurnal system (de Boer *et al.*, 1989; Archer *et al.*, 1995). Thick lamina was formed by dominant tidal current, whereas thin lamina was deposited by subordinate tidal current. A paired thick/thin laminae can be formed as a result of velocity asymmetry of flood and ebb tides in a diurnal system (Kuecher *et al.*, 1990). However, the lack of erosional contact indicating bidirectional currents as well as very fine-grained texture indicates that the silty rhythmites in Youngjong coastal area formed

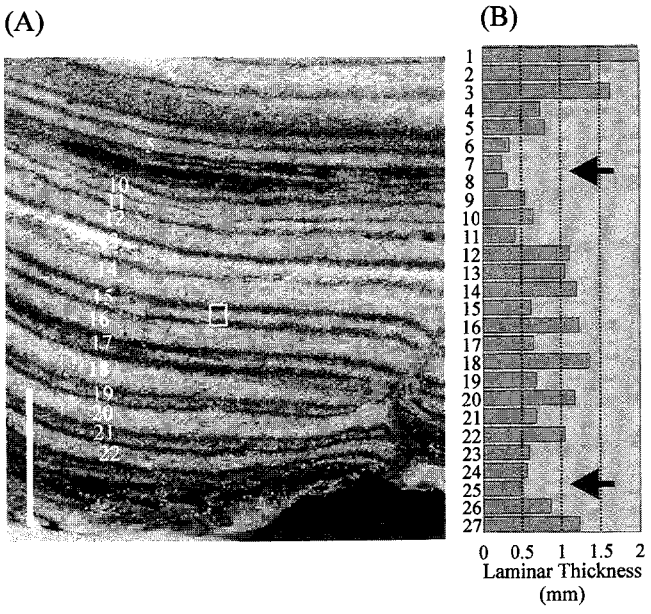

Fig. 7. (**A**) Photograph of cored sample BP1521 displaying repetitive alternation of thin/thick laminae as a couplet superimposed on overall sinusoidal variation of laminar thickness. Scale bar is 0.5 cm. Photomicrograph of box area in the middle of figure appears in Fig. 3. (**B**) Plot of laminar thickness against laminar number. Inferred neap stages are indicated by arrows. See Fig. 2 for sample location.

under relatively weak energy conditions presumably near high water level where the influence of tidal asymmetry is great. Thus, the generation of the paired laminae by each diurnal tide (flood and ebb) is unlikely.

DISCUSSION

The number of laminae in each inferred neap-spring cycle of the silty rhythmites is smaller than that of predicted high tides (28 tides) in a semidiurnal neap-spring cycle. This incomplete preservation of laminae is most likely due to laminar amalgamation of some weak tidal currents caused by the temporal change of current speed and/or geographic location of depositional site. In general, toward neap tides, the strength of tidal current decreases significantly so that the current can not afford to transport coarser particles, resulting in a prolonged suspension-deposition over many tidal cycles. Laminae become muddier and thinner, lacking distinguishable boundaries (Kvale and Archer, 1990; Miller and Eriksson, 1997). Meanwhile, weakened tidal currents may also result in nondeposition.

The relative position of the depositional site in the tidal flat system is particulary important in controlling the number of preserved laminae. In the upper level of intertidal zone where limited number of floods can approach, significantly reduced number of laminae has been observed in the modern macrotidal estuarine environment (Dalrymple *et al.*, 1991; Tessier, 1993; Archer and Johnson, 1997). Meanwhile, the proximity to sediment source also affects the number of laminae generated within a neap-spring cycle. As the distance from source channel increases, laminae become muddier and thinner due to the decrease in current strength, which significantly reduces the number of discrete laminae (Dalrymple *et al.*, 1991).

The dominance of silt-sized sediment and the lack of cross lamina and erosional contact indicate that the silty tidal rhythmites in Youngjong Island were deposited under a relatively low energy condition. Preservation of rhythmic structure as a continuous time-record suggests that wave was insignificant during sedimentation (Tessier, 1993). None to weak bioturbation probably resulted from the combinated effects of (1) high sedimentation rate enough to overcome the biological disturbances and to record continuous tidal signals and (2) drastic change in salinity unfavorable to micro- and macro-organisms for living, which is common in the estuarine intertidal flat (Howard and Frey, 1975; Dalrymple *et al.*, 1991). Corroborant evidence for subaerial exposure, such as desiccation cracks and rain-drop imprints, is absent in the studied silty tidal rhythmites, though they are common in other intertidal deposits (Dalrymple *et al.*, 1991; Kvale and Archer, 1991; Lanier *et al.*, 1993).

Sedimentation rate of the silty tidal rhythmites is estimated approximately to be 2—3 cm/mon. This value is quite high compared to those reported from modern tidal flat that are typically less than 1 cm/yr (Alexander *et al.*, 1991). This rapid and high sedimentation means that deposition of the silty rhythmites occurred locally and temporarily, probably related to rapid generation of accommodation by channel abandonment (van den Berg, 1981; Roep, 1991). The compaction of organic-rich mud deposits, 5—7 m thick, underlying the silty tidal rhythmites (Fig. 2) also seems to be partly responsible for the generation of accommodation space.

Although laminated structures are very common in the Holocene tidal deposits along the western coast of Korea (Park *et al.*, 1995), almost all of

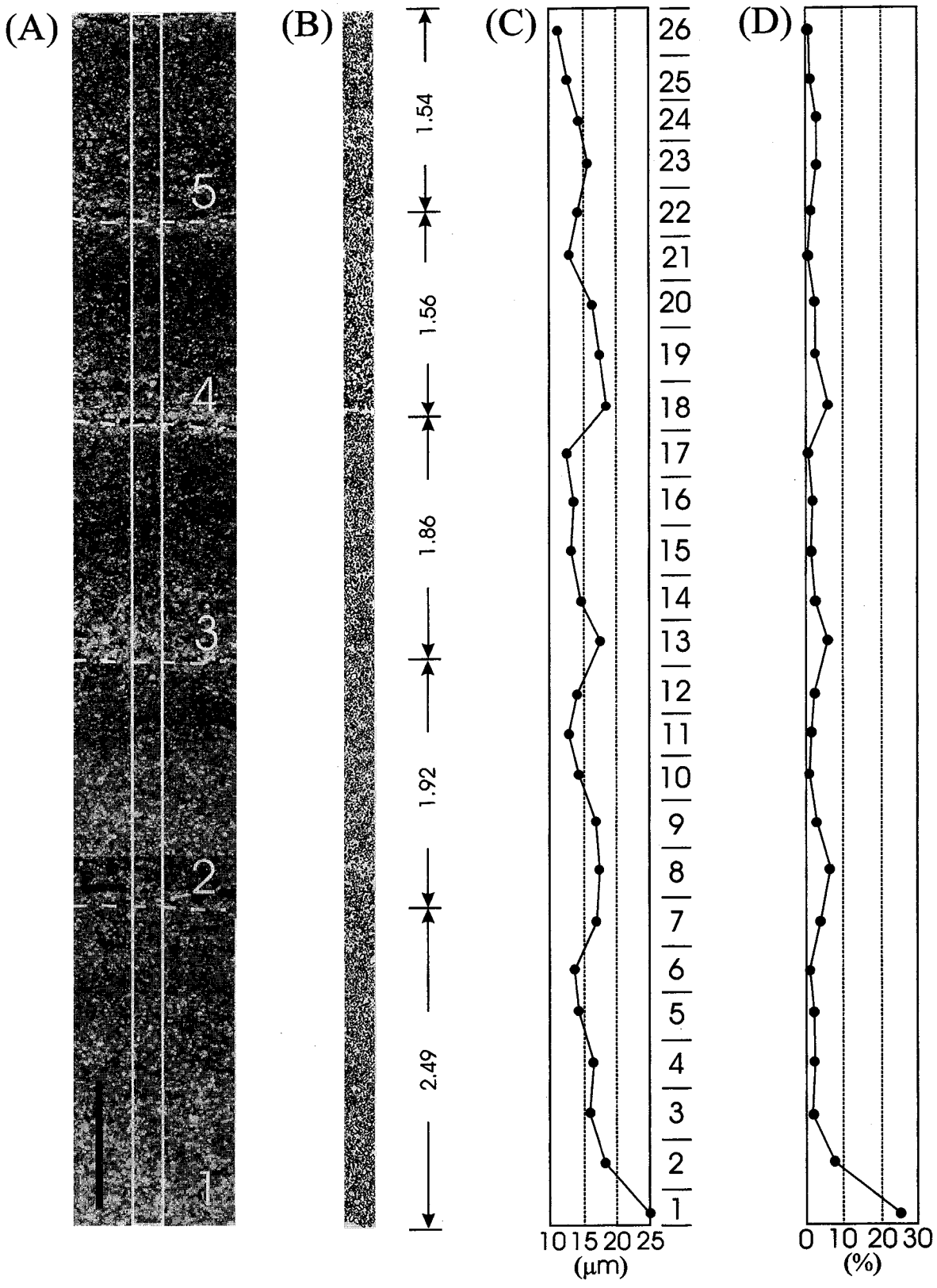

Fig. 8. (A) Photomicrograph of cored sample PT3514. Refer to Fig. 5 for location of this figure. Scale bar is 1 mm. (**B**) Line drawing of box area in (A) showing five normally graded laminae with their thickness in mm. (**C**) Vertical profile of mean grain size at 26 intervals displaying five discrete fining-upward trends. (**D**) Vertical profile of the amount (%) of 5 phi fraction (the coarsest fraction) at 26 intervals exhibiting similar trend to that of mean grain size. Note both mean grain size and the percentage of 5 ϕ fraction at each lamina decrease upwardly as lamina gets thinner.

Table 1. Summary of grain size distribution[1] and mean grain size at 26 intervals from five laminae shown in Fig. 8

Measured interval	Size (ϕ) fraction (%)				Total counts	Mean grain size (μm)
	5	6	7	8		
1	25.4	39.8	23.7	11.1	118	25.9
2	7.5	33.3	29.8	29.4	228	17.8
3	1.7	34.9	34.5	29.0	238	15.8
4	2.6	36.3	42.3	18.8	234	16.4
5	2.1	27.6	46.1	24.3	243	14.5
6	0.7	24.6	43.0	31.7	293	13.4
7	3.8	33.5	40.7	22.0	209	16.6
8	6.2	37.6	35.4	20.8	178	17.4
9	2.9	33.3	41.1	22.7	207	16.5
10	0.9	28.4	43.6	27.1	225	14.3
11	1.0	18.7	45.2	35.1	299	12.9
12	1.8	22.9	45.1	30.2	275	13.8
13	6.0	32.5	43.5	18.0	200	17.4
14	2.5	23.8	52.0	21.7	244	14.6
15	1.0	21.1	49.5	28.4	303	13.0
16	1.4	23.3	49.1	26.1	283	13.5
17	0.3	17.9	55.0	26.8	313	12.6
18	5.8	40.7	44.8	8.7	172	18.4
19	2.2	41.2	49.5	7.1	182	17.3
20	2.5	36.8	50.0	10.8	204	16.0
21	0.4	18.3	53.2	28.1	263	12.7
22	1.3	22.2	54.8	21.8	239	14.1
23	2.9	33.1	46.9	17.2	239	15.6
24	2.9	17.6	62.2	17.2	238	14.1
25	0.6	17.8	53.6	28.0	321	12.7
26	0.6	13.6	53.9	31.9	323	11.7

[1] Grains coarser than 9 ϕ (2 μm) were analyzed.

them do not exhibit tidal rhythms. The rare occurrence of tidal rhythmites in the modern tidal deposits is attributable to the intense biological and harsh physical conditions. The surfaces of modern tidal flats are dominated by dense population of benthic organisms, whereby severe bioturbation hampers the preservation of sedimentary structure (Frey *et al.*, 1989). Direct influence of strong currents and waves (associated with storm surges in winter and typhoons in summer) onto the tidal flats that are open to sea without barrier islands result in significant erosion and disturbance of coastal sediments deposited during fairweather (Park *et al.*, 1996). Considering those characters of modern tidal-flat systems, it is anticipated that ancient depositional setting of the Youngjong Island was protected and less dynamic in terms of biological activities and physical reworkings.

CONCLUSIONS

Late Pleistocene silty tidal rhythmites exhibit two types of cyclic variations in laminar thickness which are well correlated to tidal rhythms. A bundle of 12—20 laminae demonstrating sinusoidal variation in laminar thickness (Type I) is interpreted to have been formed by tidal currents during a neap-spring cycle. An alternation of thick and thin laminae as a couplet (Type II) represents diurnal inequality of asymmetric semidiurnal tides in which thick lamina was formed by dominant tidal current and thin lamina by subordinate tidal current. The silty tidal rhythmites reflect local and short-term record of rapid sedimentation without the affection of wave reworking and bioturbation.

ACKNOWLEDGEMENTS

This study was supported by a predoctorial fellowship of the Korea Research Foundation (1997) granted to Choi and partly by grant to Park from KOSEF (95-0703-0201-3). We thank Dr. Hi-Il Yi (KORDI) and an anonymous reviewer for their constructive comments on the manuscript. We also acknowledge the helpful comments of S.B. Kim.

REFERENCES

Alexander, C.R., C.A. Nittrouer, D.J. DeMaster, Y.A. Park and S.C. Park, 1990. Macrotidal mudflats of west Korea: a model for interpretation of intertidal deposits. *J. Sediment. Petrol.*, **61**: 805–824.

Archer, A.W. and T.W. Johnson, 1997. Modelling of cyclic tidal rhythmites (Carboniferous of Indiana and Kansas, Precambrian of Utah, USA) as a basis for reconstruction of intertidal positioning and paleotidal regimes. *Sedimentology*, **44**: 991–1010.

Archer, A.W., H.R. Feldman, E.P. Kvale and W.P. Lanier, 1994. Comparison of drier- to wetter-interval estuarine roof facies in the Eastern and Western Interior coal basins, USA. *Palaeogeogr. Palaeoclim. Palaeoecol.*, **106**: 171–185.

Archer, A.W., G.J. Kuecher and E.P. Kvale, 1995. The role of tidal-velocity asymmetries in the deposition of silty tidal rhythmites (Carboniferous, Eastern Interior Coal Basin, U.S. A.). *J. Sediment. Petrol.*, **65A**: 408–416.

Archer, A.W., E.P. Kvale and H.R. Johnson, 1991. Analysis of modern equatorial tidal periodicities as a test for information encoded in tidal rhythmites. In: Clastic Tidal Sedimentology, edited by Smith, D.G., G.E. Reinson, B.A. Zaitlin and R.A. Rahmani, *Can. Soc. Petrol. Geol., Mem.*, **16**: 189–196.

Brown, M.A., A.W. Archer and E.P. Kvale, 1990. Neap-spring tidal cyclicity in laminated carbonate channel-fill deposits and its implications: Salem Limestone (Mississippian), south-central basin. *J. Sediment. Petrol.*, **60**: 152–159.

Chan, E.A., E.P. Kvale, A.W. Archer and C.P. Sonett, 1994. Oldest direct evidence of lunar-solar tidal forcing encoded in sedimentary rhythmites, Proterozoic Big Cottonwood Formation, central Utah. *Geology*, **22**: 791–794.

Choi, K.S. and Y.A. Park, 1996. Lithostratigraphy and depositional environment of the coastal deposit in the Youngjong-do tidal flat, west coast of Korea. In: Abstracts of International Conference on Tidal Sedimentology, edited

by Davis, R.A. and L. Petersen, Savannah (Georgia), pp. 18.
Dalrymple, R.W. and Y. Makino, 1989. Description and genesis of a tidal bedding in the Cobequid Bay-Salmon River estuary, Bay of Fundy, Canada. In: Sedimentary Facies in the Active Plate Margin, edited by Taira, A. and F. Masuda, Terra Scientific Publication, Tokyo, pp. 151–177.
Dalrymple, R.W., Y. Makino and B.A. Zaitlin, 1991. Temporal and spatial patterns of rhythmite deposition on mud flats in the macrotidal Cobequid Bay-Salmon River estuary, Bay of Fundy, Canada. In: Clastic Tidal Sedimentology, edited by Smith, D.G., G.E. Reinson, B.A. Zaitlin and R.A. Rahmani, *Can. Soc. Petrol. Geol., Mem.*, **16**: 137–160.
de Boer, P.L., A.P. Oost and M.J. Visser, 1989. The diurnal inequality of the tides as a parameter for recognizing tidal influences. *J. Sediment. Petrol.*, **59**: 912–921.
Feldman, H.R., M.R. Gibling, A.W. Archer, W.G. Wightman and W.P. Lanier, 1995. Stratigraphic architecture of the Tonganoxie paleovalley fill (Lower Virgilian) in northeasrern Kansas. *Bull. Am. Asso. Petrol. Geol.*, **79**: 1019–1043.
Frey, R.W., J.D. Howard, S.-J. Han and B.-K. Park, 1989. Sediments and sedimentary sequences on a modern macrotidal flat, Inchon, Korea. *J. Sediment. Petrol.*, **59**: 28–44.
Greb, S.F. and A.W. Archer, 1995. Rhythmic sedimentation in a mixed tide and wave deposit, Hazel Patch Sandstone (Pennsylvanian), Eastern Kentucky Coal Field. *J. Sediment. Petrol.*, **65B**: 96–106.
Howard, J.D. and R.W. Frey, 1975. Estuaries of the Georgia coast, U.S.A.: Sedimentology and biology II. Regional animal-sediment characteristics of Georgia estuaries. *Senckenbergiana Maritima*, **7**: 33–103.
Jim, C.Y., 1985. Impregnation of moist and dry unconsolidated clay samples using Spurr resin for microstructural studies. *J. Sediment. Petrol.*, **55**: 597–599.
Kuecher, G.J., B.G. Woodland and F.M. Broadhurst, 1990. Evidence of deposition from individual tides and tidal cycles from the Francis Creek Shale (host rock to the Mazon Creek Biota), Westphalian D (Pennsylvanian), northeastern Illinois. *Sediment. Geol.*, **68**: 211–221.
Kvale, E.P. and A.W. Archer, 1990. Tidal deposits associated with low-sulfur coals, Brazil Fm. (Lower Pennsylvanian), Indiana. *J. Sediment. Petrol.*, **60**: 563–574.
Kvale, E.P. and A.W. Archer, 1991. Characteristics of two Pennsylvanian-age semi-diurnal tidal deposits in the Illinois Basin, U.S.A. In: Clastic Tidal Sedimentology, edited by Smith, D.G., G.E. Reinson, B.A. Zaitlin and R.A. Rahmani, *Can. Soc. Petrol. Geol., Mem.*, **16**: 179–188.
Kvale, E.P. and A.W. Archer, 1996. Tidal Rhythmites and Their Applications. Workshop guidebook to International Conference on Tidal Sedimentology, Savannah (Georgia), 71 pp.
Kvale, E.P., J. Cutright, D. Bilodeau, A.W. Archer, H.R. Johnson and B. Pickett, 1995. Analysis of modern tides and implications for ancient tidalites. *Cont. Shelf Res.*, **15**: 1921–1943.
Lanier, W.P., H.R. Feldman and A.W. Archer, 1993. Tidally modulated sedimentation in a fluvial to estuarine transition, Douglas Group, Missourian–Virgilian, Kansas. *J. Sediment. Petrol.*, **63**: 860–873.
Lee, C.B., Y.A. Park and C.H. Koh, 1985. Sedimentology and geochemical properties of intertidal surface sediments of the Banweol area in the southern part of Kyeonggi Bay, Korea. *J. Oceanol. Soc. Korea*, **20**: 20–29.
Miller, D.J. and K.A. Eriksson, 1997. Late Mississippian prodeltaic rhythmites in the Appalachian Basin: A hierarchical record of tidal and climatic periodicities. *J. Sediment. Petrol.*, **67**: 653–660.
Nio, S.D. and C.S. Yang, 1991. Diagnostic attributes of clastic tidal deposits: a review. In: Clastic Tidal Sedimentology, edited by Smith, D.G., G.E. Reinson, B.A. Zaitlin and R.A. Rahmani, *Can. Soc. Petrol. Geol., Mem.*, **16**: 3–28.
Park, Y.A., J.T. Wells, B.W. Kim and C.R. Alexander, 1995. Tidal lamination and facies development in the macrotidal flats of Namyang Bay, west coast of Korea. In: Tidal Signatures in Modern and Ancient Sediments, edited by Flemming, B.W. and A. Bartholoma, *Int. Asso. Sedimentol., Spec. Publ.*, **24**: 183–191.
Park, Y.A., J.H. Chang, C.H. Lee and S.J. Han, 1996. Controls of storm and typhoons on chenir formation in Komso Bay, western Korea. *J. Coast. Res.*, **12**: 814–822.
Roep, Th.B., 1991. Neap-spring cycles in a subrecent tidal channel fill (3665 BP) at Schoorldam, NW Netherlands. *Sediment. Geol.*, **71**: 213–230.
Tessier, B., 1993. Upper intertidal rhythmites in the Mont-Saint-Michel Bay (NW France); perspectives for paleoreconstruction. *Mar. Geol.*, **110**: 355–367.
Tessier, B., A.W. Archer, W.P. Lanier and H.R. Feldman, 1995. Comparison of ancient tidal rhythmites (Carboniferous of Kansas and Indiana, USA) with modern analogues (the Bay of Mont-Saint-Michel, France). In: Tidal Signatures in Modern and Ancient Sediments, edited by Flemming, B.W. and A. Bartholoma, *Int. Asso. Sedimentol., Spec. Publ.*, **24**: 259–271.
van den Berg, J.H.J., 1981. Rhythmic seasonal layering in a mesotidal channel fill sequence, Oosterschelde Mouth, the Netherlands. In: Holocene Marine Sedimentation in the North Sea Basin, edited by Nio, S.D., R.T.E. Shüttenhelm and Tj.C.E. Van Weering, *Int. Asso. Sedimentol., Spec. Publ.*, **5**: 147–159.
Williams, G.E., 1991. Upper Proterozoic tidal rhythmites, South Australia: sedimentary features, deposition, and implications for the earth's paleorotation. In: Clastic Tidal Sedimentology, edited by Smith, D.G., G.E. Reinson, B.A. Zaitlin and R.A. Rahmani, *Can. Soc. Petrol. Geol., Mem.*, **16**: 161–177.

Manuscript received April 13, 1998
Revision accepted June 12, 1998